Published in final edited form as:
J Alzheimers Dis. 2010 ; 22(4): 1313–1329. doi:10.3233/JAD-2010-101155.

MAPT Isoforms: Differential Transcriptional Profiles Related to 3R and 4R Splice Variants

Shufen Chen[a], **Kirk Townsend**[a], **Terry E. Goldberg**[a], **Peter Davies**[a,b], and **Concepcion Conejero-Goldberg**[a,*]

[a]The Litwin-Zucker Research Center for Study of Alzheimer's Disease, The Feinstein Institute for Medical Research, North Shore University Hospital, Manhasset, NY, USA

[b]Department of Pathology, Albert Einstein College of Medicine, Bronx, NY, USA

Abstract

Tau aggregation in neurofibrillary tangles is a pathological hallmark in tauopathies including Alzheimer's disease (AD). The predominant aggregation of certain MAPT (tau gene) isoforms, either the 4-repeat (4R tau) or the 3-repeat (3R tau) isoform has been widely described in tauopathies. Alterations of the 4R tau to 3R tau ratio may be a key for tau-related neurodegeneration. To study the biological consequences in expression between tau splicing isoforms 4R and 3R, we analyzed the main neurobiological effects of inclusion of the repeat region coded by exon 10 in MAPT. We compared the transcriptional profiles of the 4R tau isoforms to 3R tau isoforms using whole-genome gene expression profiling microarrays using human neuroblastoma SH-SY5Y cell lines overexpressing either human 4R tau or 3R tau isoforms. We identified 68 transcripts that differed significantly (at $p < 0.001$) between 4R and 3R isoforms as conditioned on a second variant, the so-called 2N inclusion. We extended these findings in a 2 × 2 ANOVA to examine interaction effects of these variants. Transcripts involved in embryonic development were downregulated when exon 10 was present, while transcripts related to outgrowth of neurites were generally upregulated. An important pathway implicated in AD also differed between the 3R and 4R cell lines, Wnt signaling. These studies demonstrate expression differences between MAPT isoforms 4R tau or 3R tau due to the inclusion/exclusion of the repeat region coded for by exon 10. Our data add to complex findings on the role of 3R/4R in normal and abnormal neuronal function and highlight several molecular mechanisms that might drive neurodegeneration, or perhaps, set the stage for it.

Keywords

Alzheimer's disease; gene expression profiling; microarrays; tau 3R; tau 4R

INTRODUCTION

In the adult human brain, alternative splicing of tau generates six isoforms that differ by the regulated inclusion of two inserts near the N-terminus (or their absence, hereafter 2N and 0N) and either three or four imperfect repeat regions, corresponding to the microtubule-

*Correspondence to: Concepcion Conejero-Goldberg, MD, PhD, The Litwin-Zucker Research Center for the Study of Alzheimer's Disease, The Feinstein Institute for Medical Research, 350 Community Drive, Manhasset, NY 11030, USA. Tel.: +1 516 562 3495; cgoldber@nshs.edu.

Supplementary data available online: http://www.j-alz.com/issues/22/vol22-4. html#supplementarydata05

Authors' disclosures available online (http://www.j-alz.com/disclosures/view.php?id=597).

binding domains in the C-terminal [1]. Tau isoforms containing either three (3R) or four (4R) microtubule-binding repeats are approximately equal in normal brain i.e., they are in a 50/50 ratio [2,3]. These ratios can be substantially altered in most of the neurodegenerative tauopathies: increases in the 4R to 3R ratio have been described in frontotemporal dementia, progressive supranuclear palsy, and sporadic corticobasal ganglionic degeneration [4–6]. In Alzheimer's disease (AD) an altered ratio is present due to an increase in 4R tau isoforms or decrease in 3R tau levels, and resulting in an approximately 2:1 4R:3R ratio [7, 8].

Alternative RNA splicing and phosphorylation of tau are cellular mechanisms that regulate microtubule stability. During embryonic and early developmental stages the 3R tau isoforms are predominant, while in adult human brain all six tau isoforms are present [2,3]. Increased phosphorylation occurs at embryonic stages when there is more neuronal plasticity while it is relatively reduced in adult human brain compared to that in embryonic brain. Increased tau phosphorylation reduces the amount of tau that binds to microtubules, and 3R tau isoforms also bind less tightly than 4R tau to microtubules [9]. Hyperphosphorylation of tau is thought to be pathogenic in tau-related toxicity in AD. The precise relationship between 3R:4R ratio, tau phosphorylation, tau microtubule stabilization, tau aggregation, and ultimately, cell death is unknown (see [10] for an overview). Impact of the N terminal was examined by Conrad and colleagues [8] who observed that AD-control classification was well above chance using exon 2 presence or absence in a postmortem study.

In this study, we analyzed the primary biological effects of inclusion of the imperfect repeat region coded for by exon 10 in MAPT using a human neuroblastoma cell line. When exon 10 is present, tau is considered 4R, when absent 3R. In order to further refine our analysis we conditioned 4R and 3R contrasts on N terminal presence or absence of exons 2 and 3 in tau. By comparing 4R tau isoforms to 3R tau isoforms using whole-genome gene expression profiling microarrays, we were able to comprehensively and systematically determine the downstream consequences of 4R and 3R at the level of individual transcripts and signaling pathways.

MATERIALS AND METHODS

Cell culture and stable transfection of human 4R and 3R cDNAs

Human neuroblastoma SH-SY5Y cells were maintained at 37°C and 5% CO_2, in Dulbecco's modified minimal essential medium (DMEM) (Life Technologies, Burlington, ON) supplemented with 10% (v/v) fetal bovine serum (FBS), 1% (v/v) penicillin and streptomycin (Life Technologies, Burlington, ON). SH-SY5Y cells were stable transfected with a four repeat (plasmids: pRcCMV2-Tau A and pRcCMV2-Tau C) and three repeat (plasmids: pRcCMV2-Tau B and pRcCMV2-Tau D) human tau cDNAs using Lipofectamine™ 2000 (Invitrogen, CA) as follows: cells were plated at density of 2.5×10^5 cells/well in six-well plates and grown until they reached 90% confluence. They were then transfected in serum-free medium with 10 μl of Lipofectamine plus 4μg of plasmid and left at 37°C for 5 h. After replacement of serum-free with complete medium, they were maintained for an additional 48 h, trypsinized and plated in the presence of 400 μg/mlG-418 (Invitrogen, CA) until all non-transfected cells were dead. Individual resistant colonies were picked and maintain in the presence of G-418 (200 μg/ml).

Microarray experiments

Six experiments per each condition were performed using the stably transfected SH-SY5Y cells overexpressing Tau A (4R/2N), Tau B (3R/2N), Tau C (4R/0N), and Tau D (3R/0N). As noted when exon 10 is present, tau is considered 4R, when absent 3R. Tau isoforms A and B have inclusions of two inserts near the N-terminus (exons 2 and 3), and will be

hereafter called 2N. Tau C and Tau D lack those two inserts, and are hereafter called 0N. Thus, four isoforms were included in this study (Tau A, B, C, D).

Cells were plated at a density of 3.0×10^5 cells/well in six-well plates and grown for 24 h at 37°C and 5% CO_2, in DMEM supplemented with 10% (v/v) FBS, 1% (v/v) penicillin and streptomycin. Total RNA from cell lines was extracted using standard procedures as described previously [11]. Briefly, total RNA (DNAse treated) was isolated using an RNeasy kit with a QI-Ashredder column (Quiagen) and measured for quality using Agilent 2100 Bioanalyzer (Agilent Technologies, Palo Alto, CA). RIN values in this study were ≥ 9.0. Microarrays were utilized according to the manufacturer's guidelines (Illumina). Total RNA (260 ng) was converted to cDNA by reverse transcription using ArrayScript™ reverse transcriptase and T7-Oligo $(dT)_{24}$ primers, followed by second-strand synthesis to generate double-stranded cDNA. After purification, the cDNA was converted to biotin-labeled cRNA (Totalprep™ RNA Labeling Kit, Ambion), hybridized to the microarray platform: HumanWG-6_V2 Expression BeadChip (Illumina, San Diego, CA), and stained with streptavidin-Cy3 for visualization (1.5 μg/20 μl cRNA loaded on the chip). A total of 24 microarrays were run (six experiments of neuroblastoma cells overexpressing Tau A, six overexpressing Tau B, six overexpressing Tau C, and six overexpressing Tau D).

Data preprocessing

After the probe arrays were scanned, the resulting images were first pre-processed using the BeadStudio software (Illumina, San Diego, CA), which calculates the mean fluorescence signal across all 30-replicates of each gene/transcript (AVG_Signal) along with a detection score that represents the probability that the mean signal for each gene/transcript on the chip is greater than background (i.e., detection p-value). Genes/transcripts were defined as being significantly expressed above background (as detected by the array) when each gene's detection p-value was ≤ 0.001. The expression data were then normalized within quantiles across samples of the distribution of gene expression values.

BeadStudio calculates background as the average signal intensity estimated from the negative control bead types (~700) and removes outliers using the median absolute deviation method (Illumina, BeadStudio). However, previous studies [12] and our own pilot studies indicated that background subtraction had a negative impact on data quality (e.g., it lowered correlation coefficients between technical replicates), so we therefore exported data that were normalized, but that did not undergo background subtraction. As a result of this processing 20107 of 48701 possible transcripts met quality control criteria and were used in all subsequent analyses in BRB Array Tools 3.7, a statistical software package designed for microarray analysis developed by NIH (http://linus.nci.nih.gov/BRB-ArrayTools.html).

Statistical analysis

Normalized data were imported to BRB-Array Tools and processed within the univariate module. First we examined the isoforms using a conservative Venn-type approach designed to yield robust and consistent differences between 3R and 4R isoforms. We thus conditioned 3R versus 4R contrasts on the presence or absence of 2N (i.e., 2N and 0N).We identified those transcripts which both differed significantly ($p \leq 0.001$) and differed in the same direction (i.e., up or down regulated) in the two separate 3R-4R contrasts. Thus we contrasted Tau A versus Tau B (2N present) and Tau C versus Tau D (2N absent). Six biological replicates were averaged in each group. Likelihood ratio test statistics (F test) were used to investigate the significance of the difference score between the classes i.e., an F-test was computed separately for each gene using the normalized intensities. We report p values for the class variable only. Expression differences were considered statistically significant if their p values were less than 0.001. We limited the proportion of false

discoveries using a multivariate permutation test in which the FDR was set at 0.10. We then selected the transcripts that differed significantly and in the same direction for further heat map analyses, pathway analyses, and discussion.

We also conducted a second set of parametric statistical analyses by examining the data in a 2 (3R/4R) × 2 (2N/0N) ANOVA in the BRB statistical environment using the A*B model. As a result we could detect main effects of 3R-4R isoforms, main effects of 2N-0N isoforms, and interactions.

Hierarchical clustering of expression changes

Hierarchical clustering of transcript difference scores was performed using Euclidean distance as a distance metric and complete linkage. The cluster analysis of transcripts (and cases) produced a heat map image in which the rows in the image plot represent the transcripts, and the columns in the image plot represent the neuroblastoma cell line samples.

Biological and signaling pathways analyses (*KEGG*)

Goeman's Global Test is a logistic regression model that tests the null hypothesis that there are no genes within a given set (pathway) that are differentially expressed using an exact permutation method (n = 10000) to determine an exact p value [13,14].

Real-time quantitative polymerase chain reaction (RTq-PCR)

For selected transcripts (10 genes), showing differential expression between the 3R and 4R groups, cD-NA synthesis was generated for each sample with the Ambion reverse transcription Kit and oligo dT primer. For each sample, amplified product differences were measured with two replicates with locked nucleic acid (LNA) chemistry-based detection. For housekeeping genes, primers, and probes used, see Supplementary Table 1 (available online: http://www.j-alz.com/issues/22/vol22-4.html# supplementarydata05). The RT-qPCR reactions were carried out in an ABI Prism 7900HT thermal cycler (Applied Biosystems Inc.), determining the ΔΔCt and fold changes. Statistical analysis on 3R and 4R difference scores was performed using a Student's *t*-test in Microsoft Excel.

IPA analysis: functional analysis of the 68 transcripts

We ascertained the biological significance of the transcripts found to be significant by F test and FDR (n = 68, see below) for both comparisons (Tau A vs. Tau B; Tau C vs. Tau D) using Ingenuity Pathway Analysis application (IPA/Ingenuity Systems, http://www.ingenuity.com) [15].

We first entered our transcripts of interest. Fold changes for each transcript were also included in order to refine the specificity of the analysis for both comparisons A vs. B and C vs. D. The Functional Analysis identified the biological functions and/or pathways that were most significant to the data set. Genes from the dataset that were associated with biological functions and/or pathways in the Ingenuity Pathways Knowledge Base were considered for the analysis. Fisher's exact test was used to calculate a p-value determining the probability that each biological function assigned to that data set was found by chance.

RESULTS

Transcripts differentially expressed between 4R and 3R isoforms (3R-4R contrast conditioned on 2N-0N)

In order to identify the main biological effects of 3R-4R we compared the effects of overexpressing 4R isoforms vs. 3R isoforms. We first compared transcripts differentially

expressed between a stable SH-SY5Y cell line overexpressing Tau A isoform (4R/2N) and a stable SH-SY5Y cell line overexpressing Tau B isoform (3R/2N), we called A vs. B comparison. We identified 132 differentially expressed transcripts that differed significantly (at $p < 0.001$) between A and B groups on the univariate test. The global p value for the analysis was significant ($p = 0.002$). We next compared transcripts differentially expressed between a stable SH-SY5Y cell line overexpressing Tau C isoform (4R/0N) and a stable SH-SY5Y cell line overexpressing Tau D isoform (3R/0N). We identified 112 differentially expressed transcripts that differed significantly (at $p < 0.001$) between C and D groups on the univariate test. The global p value for the analysis was significant ($p = 0.002$).

Last and critically in this conservative approach, we determined transcripts in common between both the A vs. B and the C vs. D comparisons that were also regulated in the same direction using these criteria (Figs 1 and 2).

We identified 68 transcripts corresponding to genes from RefSeq and UniGene. The 68 transcripts, their exact p values, and fold change score for both comparisons are listed in Table 1 (Differentially expressed transcripts between both comparisons A vs. B and C vs. D are listed in Tables 2 and 3 in Supplementary Material).

Hierarchical clustering of expression changes

As shown in the heat map image (Fig. 3) the hierarchical clustering of expression changes demonstrated that in the two 4R groups (A and C), 36 of the significant transcripts identified by univariate statistics demonstrated differences in expression that were associated with strong upregulation (i.e., “red” cells). The 3R groups (B and D) demonstrated downregulation for the same 36 transcripts. The reverse pattern was shown for the 32 remaining transcripts. The A and C groups and the B and D groups both demonstrated similar magnitude of expression differences. Similarly, as shown in the Fig. 1 in Supplementary Material, the clustering dendrogram indicated that 3R cells, irrespective of 2N/0N, formed one large cluster (i.e., labeled Bs and Ds), and 4R cells (labeled As and Cs) formed a second large cluster.

RT-qPCR

We validated our microarray findings in 10 transcripts that were selected from the list of 68 transcripts: CNTNAP2, DKK1, DNER, EMILIN2, FOXC1, NPY, PPP2R2C, PRKCA, ROBO2, and VIP. These transcripts were chosen on the basis of their statistical significance, role in key biological or signaling pathways, and possible relevance to AD. They are listed in Table 2, along with p value significance levels as determined by t-test and fold changes. Critically, for each and every positive finding, we found that the pattern of RT-qPCR results was consistent with that of the microarray results in terms of regional up-or down-regulation for the 4R and 3R groups. We also examined two more transcripts, AXIN2 and CTNNB1, the end products of the Wnt signaling canonical pathway for RT-qPCR (see below).

Functional analysis of the 68 transcripts: biological functions

In order to examine the biological significance of our findings we conducted a functional analysis of the interrelationships among the 68 transcripts identified as differing significantly between the 4R and 3R cell line groups on the univariate test using IPA. Results indicate that these 68 transcripts are implicated in several biological functions as follows below. These transcripts and their biological functions are listed in Table 3.

Transcripts involved in embryonic development

Of the 68 transcripts, eleven were present in the Embryonic Development biological function with Fisher’s Exact Test p values ranging from 1.52E-04 to 4.45E-02 for

subclassifications. From the eleven transcripts, one transcript (RAC2) was upregulated in the 4R isoform group with respect to the 3R isoform group, while ten transcripts were consistently downregulated in the 4R isoform group with respect to the 3R isoform group: CD9, DKK1, FOXC1, HMX2, HOXD10, LPAR1, LRP4, RET, ROBO2, and VIP. Of these ten transcripts, we selected four of them for validation by RTqPCR: DKK1, FOXC1, ROBO and VIP (see section in RT-qPCR below).

Transcripts involved in neuronal cell morphology: outgrowth of neurites

Sixteen transcripts were present in the Cell Morphology biological function with Fisher's Exact Test p values ranging from 9.84E-06 to 4.96E-02 for subclassifications. From these sixteen transcripts, seven were directly involved in outgrowth of neurites. One of the common markers for neuronal cell differentiation is the increase in neurite outgrowth. Five of these transcripts were upregulated by the 4R isoformin our study: CNT-NAP2, DNER, PPP2R2C, SGK1, and SYT13. Two of them, CD9 and RET, were downregulated.

Transcripts involved in cellular growth and proliferation

Sixteen transcripts were present in the Cellular Growth and Proliferation biological function with Fisher's Exact Test p values ranging from 4.78E-04 to 4.35E-02 for subclassifications. Of the sixteen transcripts, five were upregulated: EMILIN2, NPY, PPP2R2C, RAC2, and SIX6. Eleven transcripts were consistently downregulated in the 4R isoform group with respect to the 3R isoform group, for both comparisons: CD9, DACH1, DKK1, FOXC1, HMX2, LPAR1, LUM, PRKCA, RET, TNFAIP6, and VIP. Most of these downregulated transcripts are involved in neuronal proliferation and survival, and suggest that those functions are decreased in Tau 4R.

Transcripts involved in cell death

For the Cell Death biological function, fifteen transcripts were present with Fisher's Exact Test p values from 9.07E-04 to 4.98E-02 for subclassifications. Of the fifteen transcripts, seven transcripts were consistently upregulated in the 4R isoform group with respect to the 3R isoform group, for both comparisons: EMILIN2, MGST1, NELL1, PPP2R2B, RAC2, SCG5, and SGK1. Eight transcripts were downregulated: CD9, DACH1, DKK1, DUSP6, LPAR1, PRKCA, RET, and VIP. Four (VIP, LPAR1, RET and PRKCA) have been implicated in neuronal survival.

KEGG signaling pathways

One significant gene set was identified with Goeman's global test p values of $p < 0.002$ within the 68 differentially expressed transcripts: the Wnt signaling pathway. Significant transcripts ($p < 0.005$) that differed between 4R and 3R included: RAC2, PPP2R2B, PPP2R2C, DKK1, and PRKCA. This Kyoto pathway is of interest because has been implicated in prior studies of AD.

2 × 2 ANOVA Analysis

The ANOVA identified 102 transcripts as a main effect of the 3R-4R contrast. These are listed in Table 4. Critically, but not unexpectedly, all 68 of the genes that we identified above using our conservative Venn-type approach were included in this set of transcripts.

For the main effect of 2N-0N, we identified 56 genes that differed significantly. These are listed in Table 5. Of these genes, 52 also demonstrated 3R-4R main effect differences.

Last, 130 transcripts demonstrated an interaction effect listed in Table 6. (The majority of these also were subject to 3R-4R main effects). The interactions did not show a clear pattern.

DISCUSSION

To the best of our knowledge, this is the first study to examine the downstream consequences of 3R and 4R isoforms, controlling for the presence or absence of 2N. In this study, we focused on and demonstrated expression differences between MAPT isoforms 4R tau and 3R tau in multiple transcripts, independent of inclusion/exclusion of 2N. As based on our analytic plan sixty eight transcripts were found to be common to both 3R-4R comparisons and were also identical in direction of regulation.

Comments about specific transcripts and signaling pathways

We found consistent evidence that transcripts involved in embryonic development were downregulated in the presence of 4R isoforms, and that transcripts related to outgrowth of neurites were generally upregulated. These data suggested that inclusion of the exon 10 may play a key role in neuronal maturation. Additionally, transcripts implicated in cell proliferation and survival were usually downregulated in 4R isoforms. Our data are in agreement with previous work by Sennvik et al. [16] that established a role for 4R tau isoforms in promoting neuronal differentiation and suppressing proliferation in hippocampus using a tau knockin/knockout mouse.

Embryonic development

ROBO2 has a crucial role in axon guidance in the mammalian central nervous system. It is strongly expressed in the fetal human brain but weakly expressed in adult brain [17]. ROBO2 mediates the function of Slit proteins in guiding commissural axons of the major forebrain projections [18]. LPAR1 activation induces a range of cellular responses: cell proliferation and survival, cell migration, and cytoskeletal changes [19]. In cortical neurons, LPA signaling inhibits migration by inducing neurite retraction and growth cone collapse [20,21]. LPA signaling has also been reported to influence survival [22]. VIP protein plays a role as neuromodulator in cell growth and differentiation during neurodevelopment [23]. It has been widely shown to have a neuroprotective effect decreasing the death of neurons in a wide range of experimental models [24,25]. RET is a member of the cadherin family, and encodes one of the receptor tyrosine kinases, which are cell-surface molecules that transduce signals for cell growth and differentiation. This gene plays a crucial role in neural crest development. As the transcripts involved in embryonic development were generally downregulated in Tau 4R, this isoform may play a role in reducing neuronal growth or plasticity.

Cell morphology

SYT13, synaptotagmin XIII, is active throughout the entire synapse formation process, being involved in vesicle docking, exocytosis, and endocytosis of synaptic vesicles, and contributing to neurite extension [26]. In neuroblastoma and PC12 cells, overexpression of human synaptotagmin protein(s) increases outgrowth of neurites and plays a role in neuronal differentiation [27, 28]. PPP2R2C, protein phosphatase 2 (formerly 2A), regulatory subunit B, gamma isoform is one of the four major Ser/Thr phosphatases, and it is implicated in the negative control of cell growth and division. Overexpression of PPP2R2C promotes neurite outgrowth through the MAPK pathway, a key mediator of neuronal differentiation [29]. Contactin associated protein-like 2 (CNTNAP2) protein is a cell adhesion molecule member of the neurexin family that contains EGF repeats and laminin G domains. CNTNAP2 is a neuronal membrane protein expressed in the axonal membrane and in the somatodendritic compartment [30]. It may play a role in the local differentiation of the axon into distinct functional subdomains. Serum and glucocorticoid inducible kinase 1 (SGK1) has been shown to increase neurite outgrowth in cultured hippocampal neurons through microtubule depolarization [31]. SGK1 expression is transcriptionally regulated by the MAPK/ERK

pathway [32]. Blocking of CD9, a cell surface glycoprotein that participates in growth and differentiation in the nervous system, has been shown to promote neurite outgrowth [33]. This complex pattern of results may be consistent with increased neuronal outgrowth when 4R isoform is present.

Cell proliferation

Of the 4R upregulated transcripts, the neuropeptide Y(NPY) is widely expressed in the central nervous system and has recently been shown to stimulate neurogenesis in the hippocampus and subventricular zone. Intracerebroventricular injection of NPY stimulates proliferation of neural precursors in the mice dentate gyrus and in the subventricular zone, and promotes differentiation of neuronal progenitors in adult mice *in vivo* [34, 35]. In neuroblastoma cell lines, NPY protein has been shown to decrease in a dose-dependent manner proliferation [36]. Another upregulated transcript was RAC2. This gene has been implicated in axon growth, guidance and dendrite spine formation and maintenance [37,38]. Rho GTPases are essential regulators of cytoskeletal reorganization during neuronal morphogenesis. Activation of the non-canonical Wnt pathway through disheveled, RAC and JNK affects dendritic development [39]. Our data suggest that the non-canonical wnt pathway is regulated by the presence/absence of tau exon 10 through the activation of RAC2 (see below KEGG signaling pathway).

Cell death

The data also suggest a complex role for 3R-4R differences in the cell death process. At the level of individual transcripts involved in cell death, EMILIN2, MGST1, NELL1, PPP2R2B, RAC2, SCG5, and SGK1 were upregulated in 4R, while some transcripts implicated in neuronal survival processes were downregulated (e.g., VIP, LPAR1, RET, and PRKCA).

To summarize, transcripts involved in cellular growth and proliferation were generally downregulated in 4R isoforms while transcripts involved in neurite outgrowth were generally upregulated. Exon 10 thus may diminish proliferation and survival while increasing neurite outgrowth. Additionally cell death transcripts involved in neuronal survival were downregulated in 4R tau, in concordance with our results.

A major pathway that was differentially activated by depending on 3R or 4R status was the Wnt/β-catenin signaling implicated in AD. Wnt proteins can signal through disheveled (Dvl): 1) to inhibit GSK-3β (canonical pathway); 2) to regulate RAC (non-canonical pathway); or 3) to activate a Ca^{2+} dependent pathway (non-canonical pathway). For the canonical pathway β-catenin mediated transcriptional activation is involved; for the non-canonical pathway RAC and Ca^{2+} signaling are involved. If the canonical pathway was activated we would be able to detect increased expression of the Wnt canonical pathway main products, β-catenin and the endogenous target gene Axin2 [40]. We conducted RT-qPCR for β-catenin andAxin2 in order to determine if differential expression between 4R and 3R isoforms was present (Table 2). Our results were consistent with the microarray study in which we showed no significant differences for both genes between isoforms 4R and 3R, suggesting no activation of the final products of the Wnt canonical pathway. While activation of the canonical Wnt pathway does not affect dendritic development, activation of the non-canonical Wnt pathway through disheveled, RAC and JNK does so [39]. Our data suggest involvement of the wnt non-canonical pathway regulated by the presence/absence of exon 10 through the activation of RAC2. The Rho family of GTPases including RAC2, play an important role in various aspects of neuronal development such as neurite outgrowth and differentiation, axon pathfinding, and dendritic spine formation and maintenance [38]. Thus, our data suggest that 4R isoforms engage the non-canonical wnt signaling pathway, perhaps

through RAC2. This pathway may affect dendritic development through disheveled, RAC, and JNK.

Nevertheless, the relatively large number of transcripts that were involved in neurodevelopment and maturation was unexpected. We had predicted that the majority of our findings would involve transcripts or pathways ostensibly involved in neurodegeneration. When we compared our findings to a postmortem brain microarray study of tauopathies we found a single gene in common (FOXC1) [41]. When we contrasted our results to a postmortem microarray study that examined tangle bearing neurons in AD [42] we did not find any genes in common.

Our study is also subject to a number of technical limitations. We used a neuroblastoma cell culture, which may yield slightly different results than if primary cultured neurons were used. For the sake of incisive experimental design we used cells which produced either 3R or 4R isoforms, which may not fully reflect more subtle differences in 3R/4R ratios *in vivo*. Additionally, our FDR approach was conservative, based on presumptive independence among all probes.

In conclusion, this study demonstrated that expression differences between 4R tau and 3R tau isoforms are present independent of the inclusion/exclusion of 2N (exons 2–3). Our data add to complex findings on the role of 3R/4R in normal and abnormal neuronal function and highlight several molecular mechanisms that might drive neurodegeneration, or perhaps, set the stage for it.

Supplementary Material

Refer to Web version on PubMed Central for supplementary material.

Acknowledgments

This research was supported by The Litwin-Zucker Research Center for Study of Alzheimer's Disease. Analysis was performed using BRB ArrayTools developed by Dr. Richard Simon and Amy Peng, Molecular Statistics and Bioinformatics Section, National Cancer Institute. We also thank Dr. Franak Batliwalla and Ms. Aarti Damle, members of the Feinstein Institute's microarray core facility, for their assistance.

REFERENCES

1. Goedert M, Wischik CM, Crowther RA, Walker JE, Klug A. Cloning and sequencing of the cDNA encoding a core protein of the paired helical filament of Alzheimer disease: identification as the microtubule-associated protein tau. Proc Natl Acad Sci U S A. 1988; 85:4051–4055. [PubMed: 3131773]
2. Goedert M, Spillantini MG, Jakes R, Rutherford D, Crowther RA. Multiple isoforms of human microtubule-associated protein tau: sequences and localization in neurofibrillary tangles of Alzheimer's disease. Neuron. 1989; 3:519–526. [PubMed: 2484340]
3. Kosik KS, Orecchio LD, Bakalis S, Neve RL. Developmentally regulated expression of specific tau sequences. Neuron. 1989; 2:1389–1397. [PubMed: 2560640]
4. Hutton M, Lendon CL, Rizzu P, Baker M, Froelich S, Houlden H, Pickering-Brown S, Chakraverty S, Isaacs A, Grover A, Hackett J, Adamson J, Lincoln S, Dickson D, Davies P, Petersen RC, Stevens M, de Graaff E, Wauters E, van Baren J, Hillebrand M, Joosse M, Kwon JM, Nowotny P, Che LK, Norton J, Morris JC, Reed LA, Trojanowski J, Basun H, Lannfelt L, Neystat M, Fahn S, Dark F, Tannenberg T, Dodd PR, Hayward N, Kwok JB, Schofield PR, Andreadis A, Snowden J, Craufurd D, Neary D, Owen F, Oostra BA, Hardy J, Goate A, van Swieten J, Mann D, Lynch T, Heutink P. Association of missense and 5'-splice-site mutations in tau with the inherited dementia FTDP-17. Nature. 1998; 393:702–705. [PubMed: 9641683]

5. Spillantini MG, Murrell JR, Goedert M, Farlow MR, Klug A, Ghetti B. Mutation in the tau gene in familial multiple system tauopathy with presenile dementia. Proc Natl Acad Sci U S A. 1998; 95:7737–7741. [PubMed: 9636220]
6. Ingelsson M, Ramasamy K, Russ C, Freeman SH, Orne J, Raju S, Matsui T, Growdon JH, Frosch MP, Ghetti B, Brown RH, Irizarry MC, Hyman BT. Increase in the relative expression of tau with four microtubule binding repeat regions in frontotemporal lobar degeneration and progressive supranuclear palsy brains. Acta Neuropathol. 2007; 114:471–479. [PubMed: 17721707]
7. Ginsberg SD, Che S, Counts SE, Mufson EJ. Shift in the ratio of three-repeat tau and four-repeat tau mRNAs in individual cholinergic basal forebrain neurons in mild cognitive impairment and Alzheimer's disease. J Neurochem. 2006; 96:1401–1408. [PubMed: 16478530]
8. Conrad C, Zhu J, Conrad C, Schoenfeld D, Fang Z, Ingelsson M, Stamm S, Church G, Hyman BT. Single molecule profiling of tau gene expression in Alzheimer's disease. J Neurochem. 2007; 103:1228–1236. [PubMed: 17727636]
9. Butner KA, Kirschner MW. Tau protein binds to microtubules through a flexible array of distributed weak sites. J Cell Biol. 1991; 115:717–730. [PubMed: 1918161]
10. Avila J. Intracellular and extracellular tau. Front Neurosci. 2010; 4:49. [PubMed: 20661459]
11. Conejero-Goldberg C, Wang E, Yi C, Goldberg TE, Jones-Brando L, Marincola FM, Webster MJ, Torrey EF. Infectious pathogen detection arrays: viral detection in cell lines and postmortem brain tissue. Biotechniques. 2005; 39:741–751. [PubMed: 16312221]
12. Barnes M, Freudenberg J, Thompson S, Aronow B, Pavlidis P. Experimental comparison and cross-validation of the Affymetrix and Illumina gene expression analysis platforms. Nucleic Acids Res. 2005; 33:5914–5923. [PubMed: 16237126]
13. Goeman JJ, van de Geer SA, de Kort F, van Houwelingen HC. A global test for groups of genes: testing association with a clinical outcome. Bioinformatics. 2004; 20:93–99. [PubMed: 14693814]
14. Goeman JJ, Oosting J, Cleton-Jansen AM, Anninga JK, van Houwelingen HC. Testing association of a pathway with survival using gene expression data. Bioinformatics. 2005; 21:1950–1957. [PubMed: 15657105]
15. Calvano SE, Xiao W, Richards DR, Felciano RM, Baker HV, Cho RJ, Chen RO, Brownstein BH, Cobb JP, Tschoeke SK, MillerGraziano C, Moldawer LL, Mindrinos MN, Davis RW, Tompkins RG, Lowry SF. Inflamm and Host Response to Injury Large Scale Collab. Res P. A network-based analysis of systemic inflammation in humans. Nature. 2005; 437:1032–1037. [erratum appears in Nature. 2005 Dec 1;438(7068):696]. [PubMed: 16136080]
16. Sennvik K, Boekhoorn K, Lasrado R, Terwel D, Verhaeghe S, Korr H, Schmitz C, Tomiyama T, Mori H, Krugers H, Joels M, Ramakers GJ, Lucassen PJ, Van Leuven F. Tau4R suppresses proliferation and promotes neuronal differentiation in the hippocampus of tau knockin/knockout mice. FASEB J. 2007; 21:2149–2161. [PubMed: 17341679]
17. Yue Y, Grossmann B, Galetzka D, Zechner U, Haaf T. Isolation and differential expression of two isoforms of the ROBO2/Robo2 axon guidance receptor gene in humans and mice. Genomics. 2006; 88:772–778. [PubMed: 16829019]
18. Long H, Sabatier C, Ma L, Plump A, Yuan W, Ornitz DM, Tamada A, Murakami F, Goodman CS, Tessier-Lavigne M. Conserved roles for Slit and Robo proteins in midline commissural axon guidance. Neuron. 2004; 42:213–223. [PubMed: 15091338]
19. Choi JW, Herr DR, Noguchi K, Yung YC, Lee C, Mutoh T, Lin M, Teo ST, Park KE, Mosley AN, Chun J. LPA Receptors: Subtypes and Biological Actions. Annu. Rev. Pharmacol. Toxicol. 2010; 50:157–186. [PubMed: 20055701]
20. Fukushima N, Weiner JA, Kaushal D, Contos JJ, Rehen SK, Kingsbury MA, Kim KY, Chun J. Lysophosphatidic acid influences the morphology and motility of young, post-mitotic cortical neurons. Mol Cell Neurosci. 2002; 20:271–282. [PubMed: 12093159]
21. Tigyi G, Fischer DJ, Sebok A, Yang C, Dyer DL, Miledi R. Lysophosphatidic acid-induced neurite retraction in PC12 cells: control by phosphoinositide-Ca2+ signaling and Rho. J Neurochem. 1996; 66:537–548. [PubMed: 8592123]
22. Zheng ZQ, Fang XJ, Qiao JT. Dual action of lysophosphatidic acid in cultured cortical neurons: survival and apoptogenic. Sheng Li Hsueh Bao. 2004; 56:163–171.

23. Muller JM, Lelievre V, Becq-Giraudon L, Meunier AC. VIP as a cell-growth and differentiation neuromodulator role in neurodevelopment. Mol Neurobiol. 1995; 10:115–134. [PubMed: 7576303]
24. Wu D. Neuroprotection in experimental stroke with targeted neurotrophins. NeuroRx. 2005; 2:120–128. [PubMed: 15717063]
25. Brenneman DE. Neuroprotection: a comparative view of vasoactive intestinal peptide and pituitary adenylate cyclase-activating polypeptide. Peptides. 2007; 28:1720–1726. [PubMed: 17513014]
26. Detrait ER, Yoo S, Eddleman CS, Fukuda M, Bittner GD, Fishman HM. Plasmalemmal repair of severed neurites of PC12 cells requires Ca(2+). and synaptotagmin. J Neurosci Res. 2000; 62:566–573. [PubMed: 11070500]
27. Di Giovanni S, De Biase A, Yakovlev A, Finn T, Beers J, Hoffman EP, Faden AI. In Vivo and in Vitro Characterization of Novel Neuronal Plasticity Factors Identified following Spinal Cord Injury. J Biol Chem. 2005; 280:2084–2091. [PubMed: 15522871]
28. Fukuda M, Mikoshiba K. Expression of synaptotagmin I or II promotes neurite outgrowth in PC12 cells. Neurosci Lett. 2000; 295:33–36. [PubMed: 11078930]
29. Strack S. Overexpression of the protein phosphatase 2A regulatory subunit Bgamma promotes neuronal differentiation by activating the MAP kinase (MAPK) cascade. J Biol Chem. 2002; 277:41525–41532. [PubMed: 12191994]
30. Bel C, Oguievetskaia K, Pitaval C, Goutebroze L, Faivre-Sarrailh C. Axonal targeting of Caspr2 in hippocampal neurons via selective somatodendritic endocytosis. J Cell Sci. 2009; 122:3403–3413. [PubMed: 19706678]
31. Yang YC, Lin CH, Lee EH. Serum- and glucocorticoid-inducible kinase 1 (SGK1) increases neurite formation through microtubule depolymerization by SGK1 and by SGK1 phosphorylation of tau. Mol Cell Biol. 2006; 26:8357–8370. [PubMed: 16982696]
32. Mizuno H, Nishida E. The ERK MAP kinase pathway mediates induction of SGK (serum- and glucocorticoid-inducible kinase) by growth factors. Genes Cells. 2001; 6:261–268. [PubMed: 11260269]
33. Banerjee SA, Hadjiargyrou M, Patterson PH. An antibody to the tetraspan membrane protein CD9 promotes neurite formation in a partially alpha3beta1 integrin-dependent manner. J Neurosci. 1997; 17:2756–2765. [PubMed: 9092597]
34. Decressac M, Wright B, David B, Tyers P, Jaber M, Barker RA, Gaillard A. Exogenous neuropeptide Y promotes in vivo hippocampal neurogenesis. Hippocampus. 2010 in press.
35. Decressac M, Prestoz L, Veran J, Cantereau A, Jaber M, Gaillard A. Neuropeptide Y stimulates proliferation, migration and differentiation of neural precursors from the subventricular zone in adult mice. Neurobiol Dis. 2009; 34:441–449. [PubMed: 19285132]
36. Reubi JC, Gugger M, Waser B, Schaer JC. Y(1)-mediated effect of neuropeptide Y in cancer: breast carcinomas as targets. Cancer Res. 2001; 61:4636–4641. [PubMed: 11389101]
37. Ng J, Nardine T, Harms M, Tzu J, Goldstein A, Sun Y, Dietzl G, Dickson BJ, Luo L. Rac GTPases control axon growth, guidance and branching. Nature. 2002; 416:442–447. [PubMed: 11919635]
38. Govek EE, Newey SE, Van Aelst L. The role of the Rho GTPases in neuronal development. Genes Dev. 2005; 19:1–49. [PubMed: 15630019]
39. Rosso SB, Sussman D, Wynshaw-Boris A, Salinas PC. Wnt signaling through Dishevelled, Rac and JNK regulates dendritic development. Nat Neurosci. 2005; 8:34–42. [PubMed: 15608632]
40. Jho EH, Zhang T, Domon C, Joo CK, Freund JN, Costantini F. Wnt/beta-catenin/Tcf signaling induces the transcription of Axin2, a negative regulator of the signaling pathway. Mol Cell Biol. 2002; 22:1172–1183. [PubMed: 11809808]
41. Bronner IF, Bochdanovits Z, Rizzu P, Kamphorst W, Ravid R, van Swieten JC, Heutink P. Comprehensive mRNA expression profiling distinguishes tauopathies and identifies shared molecular pathways. PLoS ONE. 2009; 4:e6826. [PubMed: 19714246]
42. Dunckley T, Beach TG, Ramsey KE, Grover A, Mastroeni D, Walker DG, LaFleur BJ, Coon KD, Brown KM, Caselli R, Kukull W, Higdon R, McKeel D, Morris JC, Hulette C, Schmechel D, Reiman EM, Rogers J, Stephan DA. Gene expression correlates of neurofibrillary tangles in Alzheimer's disease. Neurobiol Aging. 2006; 27:1359–1371. [PubMed: 16242812]

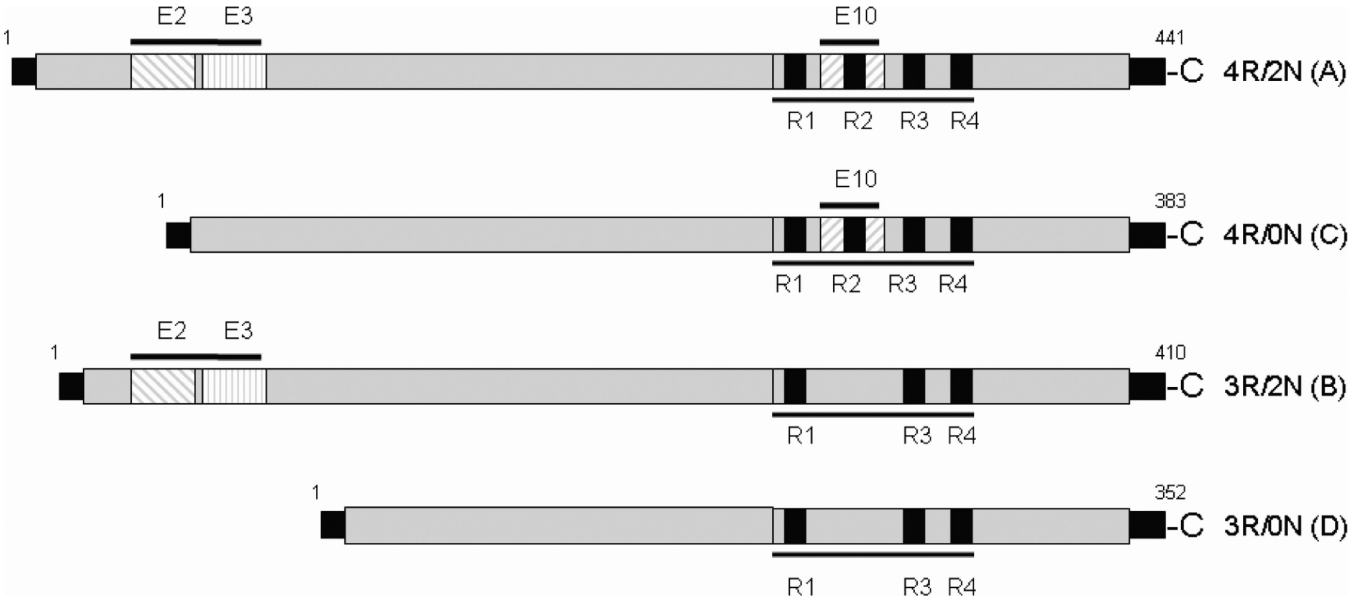

Fig. 1.
Tau isoforms overexpressed on SH-SY5Y cell lines. Tau 4R (A and C) and Tau 3R (B and D).

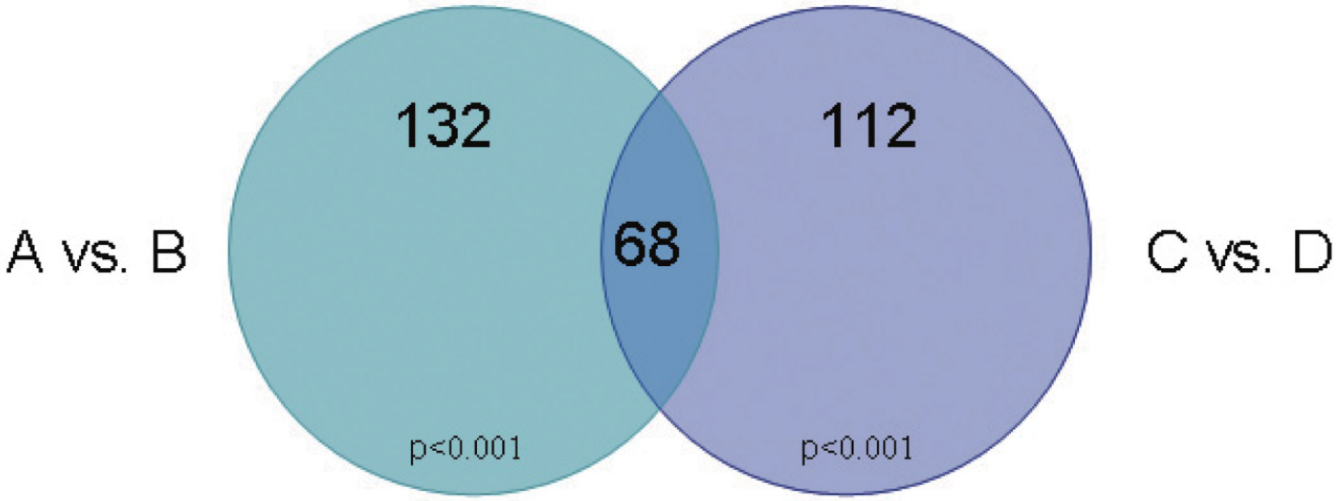

Fig. 2.

Transcripts Differentially Expressed Due to Exon 10: Venn diagram of comparisons A vs. B and C vs. D. Left circle: A vs. B comparison identifying 132 transcripts differentially expressed that differed significantly (at $p < 0.001$) between A and B groups on the univariate test. Right circle: C vs. D comparison identifying 112 transcripts differentially expressed that differed significantly (at $p < 0.001$) between C and D groups on the univariate test. Overlapping area: 68 transcripts in common between both comparisons: A vs. B and C vs. D that were also regulated in the same direction of up or down-regulated.

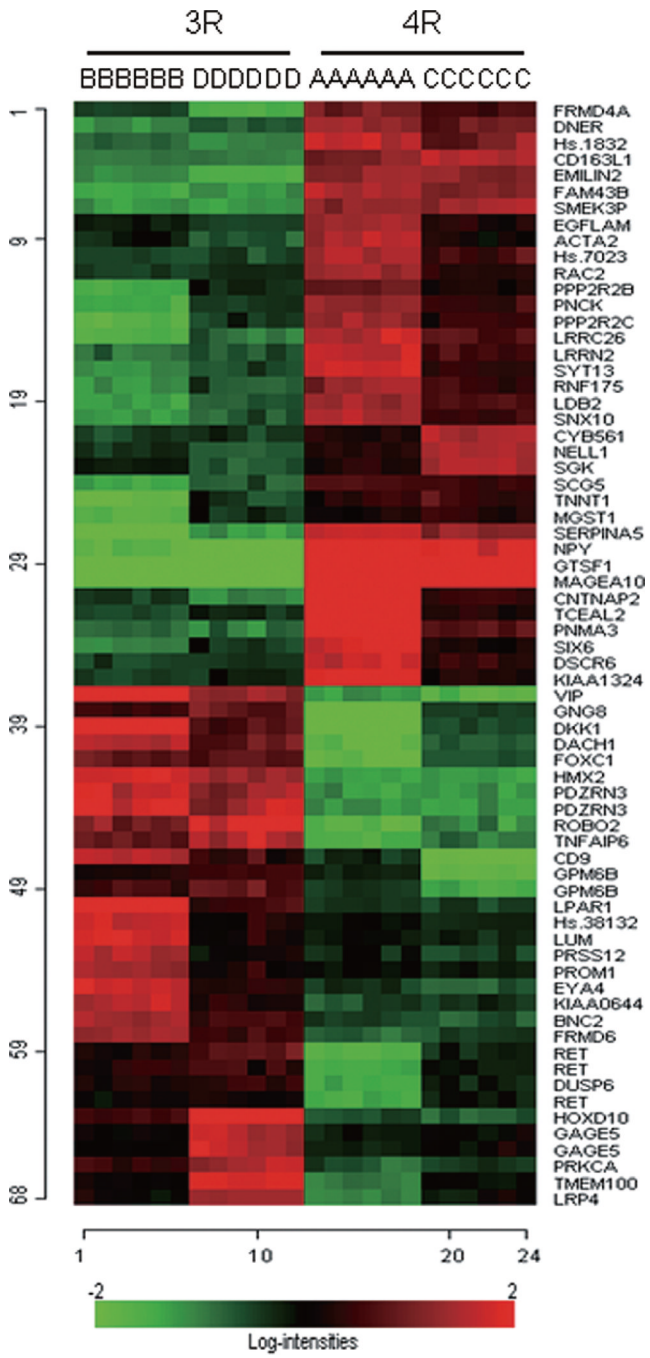

Fig. 3.

Heat map showing up-and down-regulation for the 68 transcripts identified as significant between the two 4R groups (A and C) and the 3R groups (B and D). The 68 transcripts identified as significant (all p-values < 0.001) in the univariate analysis are on the y axis and cell lines overexpressing tau isoforms are one the x axis. Log intensities of 68 transcripts are represented in colored cells. Red cells indicate relatively strong upregulation for the transcripts in that particular cell line overexpressing the tau 4R or tau 3R, whereas green cells indicate the converse.

Table 1

Transcripts differentially expressed in common between both A vs. B and C vs. D comparisons

RefSeq transcript ID	Gene symbol	Entrez Gene name	Fold change (A vs. B)	Parametric p-value	Fold change (C vs. D)	Parametric p-value
NM_001613	ACTA2	actin, alpha 2, smooth muscle, aorta	2.59	< 1e-07	1.59	< 1e-07
NM_017637	BNC2	basonuclin 2	−2.86	< 1e-07	−2.03	< 1e-07
NM_174941	CD163L1	CD163 molecule-like 1	3.10	< 1e-07	4.07	< 1e-07
NM_001769	CD9	CD9 molecule	−2.94	< 1e-07	−4.09	< 1e-07
NM_014141	CNTNAP2	contactin associated protein like 2	13.44	< 1e-07	2.38	< 1e-07
NM_001915	CYB561	cytochrome b-561	1.52	< 1e-07	2.83	< 1e-07
NM_080760	DACH1	dachshund homolog 1 (Drosophila)	−6.67	< 1e-07	−2.38	< 1e-07
NM_012242	DKK1	dickkopf homolog 1 (Xenopus laevis)	−14.29	< 1e-07	−2.01	< 1e-07
NM_139072	DNER	delta/notch-like EGF repeat	3.87	< 1e-07	2.40	< 1e-07
NM_018962	DSCR6	Down syndrome critical region gene 6	3.51	< 1e-07	1.56	< 1e-07
NM_001946	DUSP6	dual specificity phosphatase 6	−2.50	< 1e-07	−1.43	2.00E-07
NM_182801	EGFLAM	EGF-like, fibronectin III and laminin	2.39	< 1e-07	1.55	< 1e-07
NM_032048	EMILIN2	elastin microfibril interfacer 2	3.65	< 1e-07	4.52	< 1e-07
NM_004100	EYA4	eyes absent homolog 4 (Drosophila)	−3.23	< 1e-07	−1.81	< 1e-07
NM_207334	FAM43B	family with sequence similarity 43,B	4.99	< 1e-07	3.52	< 1e-07
NM_001453	FOXC1	forkhead box C1	−4.76	< 1e-07	−2.18	< 1e-07
NM_018027	FRMD4A	FERM domain containing 4A	2.33	< 1e-07	3.28	< 1e-07
NM_152330	FRMD6	FERM domain containing 6	−3.33	< 1e-07	−1.73	< 1e-07
NM_001475	GAGE5	G antigen 5	−1.14	0.0002161	−2.34	< 1e-07
NM_001475	GAGE5	G antigen 5	−1.15	0.0007225	−2.34	< 1e-07
NM_033258	GNG8	guanine nucleotide binding protein, 8	−7.69	< 1e-07	−2.10	< 1e-07
NM_001001995	GPM6B	glycoprotein M6B	−1.70	< 1e-07	−3.73	< 1e-07
NM_001001995	GPM6B	glycoprotein M6B	−1.32	1.00E-07	−3.49	< 1e-07
NM_144594	GTSF1	gametocyte specific factor 1	15.14	< 1e-07	15.35	< 1e-07
NM_005519	HMX2	H6 family homeobox 2	−5.56	< 1e-07	−4.28	< 1e-07
NM_002148	HOXD10	homeobox D10	−1.89	< 1e-07	−5.71	< 1e-07
AB073882	Hs.1832	human neuroblastoma cDNA	3.89	< 1e-07	3.08	< 1e-07

RefSeq transcript ID	Gene symbol	Entrez Gene name	Fold change (A vs. B)	Parametric p-value	Fold change (C vs. D)	Parametric p-value
BX100246	Hs.38132	Soares fetal liver spleen 1NFLS	−2.70	< 1e-07	−1.28	3.15E-05
BX537518	Hs.7023	H.S. mRNA; cDNA DKFZp686N1989	3.05	< 1e-07	1.85	< 1e-07
NM_014817	KIAA0644	KIAA0644 gene product	−3.33	< 1e-07	−1.45	1.00E-07
NM_020775	KIAA1324	KIAA1324	4.04	< 1e-07	1.30	1.81E-05
NM_001290	LDB2	LIM domain binding 2	4.39	< 1e-07	2.13	< 1e-07
NM_057159	LPAR1	lysophosphatidic acid receptor 1	−4.76	< 1e-07	−1.76	< 1e-07
NM_002334	LRP4	LDL receptor-related protein 4	−1.85	< 1e-07	−2.21	< 1e-07
NM_001013653	LRRC26	leucine rich repeat containing 26	5.94	< 1e-07	2.46	< 1e-07
NM_201630	LRRN2	leucine rich repeat neuronal 2	4.13	< 1e-07	1.95	< 1e-07
NM_002345	LUM	lumican	−2.94	< 1e-07	−1.27	6.91E-05
NM_021048	MAGEA10	melanoma antigen family A, 10	16.37	< 1e-07	15.06	< 1e-07
NM_145764	MGST1	microsomal glutath. S-transferase 1	2.83	< 1e-07	1.48	6.00E-07
NM_006157	NELL1	NEL-like 1 (chicken)	1.44	< 1e-07	3.43	< 1e-07
NM_000905	NPY	neuropeptide Y	9.93	< 1e-07	15.57	< 1e-07
XM 001133042	PDZRN3	PDZ domain containing RING finger 3	−5.26	< 1e-07	−4.54	< 1e-07
XM 001133042	PDZRN3	PDZ domain containing RING finger 3	−5.55	< 1e-07	−4.00	< 1e-07
NM_001039582	PNCK	preg. up-reg non-ubiq. CaM kinase	4.46	< 1e-07	1.62	< 1e-07
NM_013364	PNMA3	paraneoplastic antigen MA3	5.68	< 1e-07	2.55	< 1e-07
NM_181676	PPP2R2B	protein phosphatase 2, subunit B, β	3.65	< 1e-07	1.29	1.93E-05
NM_181876	PPP2R2C	protein phosphatase 2, subunit B, γ	5.33	< 1e-07	1.62	< 1e-07
NM_002737	PRKCA	protein kinase C, alpha	−1.89	< 1e-07	−2.89	< 1e-07
NM_006017	PROM1	prominin 1	−2.22	< 1e-07	−1.24	0.0001516
NM_003619	PRSS12	protease, serine, 12	−2.63	< 1e-07	−1.41	7.00E-07
NM_002872	RAC2	ras-related C3 botulinum toxin sub. 2	2.83	< 1e-07	1.43	< 1e-07
NM_020975	RET	ret proto-oncogene, variant 2	−2.38	< 1e-07	−1.81	< 1e-07
NM_020630	RET	ret proto-oncogene, variant 4	−2.70	< 1e-07	−1.43	2.40E-06
NM_020975	RET	ret proto-oncogene, variant 2	−2.86	< 1e-07	−1.20	0.000377
NM_173662	RNF175	ring finger protein 175	4.03	< 1e-07	1.92	< 1e-07
NM_002942	ROBO2	roundabout, axon guidance recept, 2	−4.76	< 1e-07	−5.85	< 1e-07
NM_003020	SCG5	secretogranin V (7B2 protein)	3.09	< 1e-07	1.99	< 1e-07

RefSeq transcript ID	Gene symbol	Entrez Gene name	Fold change (A vs. B)	Parametric p-value	Fold change (C vs. D)	Parametric p-value
NM_000624	SERPINA5	serpin peptidase inhibitor, clade A, 5	9.89	< 1e-07	3.90	< 1e-07
NM_005627	SGK1	serum/glucocorticoid regulat-kinase 1	1.27	1.00E-06	3.41	< 1e-07
NM_007374	SIX6	SIX homeobox 6	5.08	< 1e-07	1.39	5.40E-06
NR_002784	SMEK3P	SMEK homolog 3	3.89	< 1e-07	4.33	< 1e-07
NM_013322	SNX10	sorting nexin 10	4.50	< 1e-07	1.95	< 1e-07
NM_020826	SYT13	synaptotagmin XIII	5.05	< 1e-07	1.73	< 1e-07
NM_080390	TCEAL2	transcription elongation factor A	7.28	< 1e-07	1.38	5.00E-07
NM_018286	TMEM100	transmembrane protein 100	−1.79	< 1e-07	−2.89	< 1e-07
NM_007115	TNFAIP6	tumor necrosis factor, α-ind. protein 6	−3.70	< 1e-07	−3.93	< 1e-07
NM_003283	TNNT1	troponin T type 1 (skeletal, slow)	3.62	< 1e-07	1.72	1.00E-07
NM_194435	VIP	vasoactive intestinal peptide	−20.00	< 1e-07	−5.24	< 1e-07

Table 2

RT-qPCR p-values and fold changes for twelve transcripts

RefSeq transcript ID	Gene symbol	Fold change Microarray (A vs. B)	Parametric p-value	Fold change Microarray (C vs. D)	Parametric p-value	Fold change RT-qPCR (A vs. B)	Parametric p-value	Fold change RT-qPCR (C vs. D)	Parametric p-value
NM_014141	CNTNAP2	13.44	< 1e-07	2.38	< 1e-07	30.50	5.98E-06	4.50	0.00041961
NM_012242	DKK1	−14.29	< 1e-07	−2.01	< 1e-07	−25.00	0.002791324	−1.63	0.008044056
NM_139072	DNER	3.87	< 1e-07	2.40	< 1e-07	43.60	1.42567E-06	6.55	< 1e-07
NM_032048	EMILIN2	3.65	< 1e-07	4.52	< 1e-07	6.18	0.000289114	11.08	< 1e-07
NM_001453	FOXC1	−4.76	< 1e-07	−2.18	< 1e-07	−5.20	< 1e-07	−1.42	0.000207761
NM_000905	NPY	9.93	< 1e-07	15.57	< 1e-07	16.79	< 1e-07	28.54	< 1e-07
NM_181876	PPP2R2C	5.33	< 1e-07	1.62	< 1e-07	11.58	0.001891617	2.55	0.000132606
NM_002737	PRKCA	−1.89	< 1e-07	−2.89	< 1e-07	−1.58	0.000433749	−2.70	< 1e-07
NM_002942	ROBO2	−4.76	< 1e-07	−5.85	< 1e-07	−33.30	< 1e-07	−12.50	< 1e-07
NM_194435	VIP	−20.00	< 1e-07	−5.24	< 1e-07	−50.00	< 1e-07	−16.66	1.56897E-07
NM_004655	AXIN2	1.09	0.02	−1.00	0.69	1.16	0.10	1.01	0.92
NM_001904	CTNNB1	1.06	0.45	−1.06	0.71	−1.75	0.01	1.26	0.11

Table 3

Biological functions as determined by 3R/4R contrast conditioned by 2N/0N

	Embryonic development	Neuronal cell morphology	Cellular growth proliferation	Cell death
p-value	1.52E-04-4.45E-02	9.84E-06-4.96E-02	4.78E-04-4.35E-02	9.07E-04-4.98E-02
Molecules	RAC2	CNTNAP2	NPY	NELL1
	LRP4	SGK1	RAC2	MGST1
	LPAR1	SYT13	EMILIN2	RAC2
	CD9	TNNT1	VIP	SGK1
	ROBO2	DNER	HMX2	EMILIN2
	DKK1	ACTA2	FOXC1	DUSP6
	VIP	VIP	CD9	VIP
	HMX2	CD9	LPAR1	LPAR1
	RET	LPAR1	LUM	CD9
	FOXC1	SERPINA5	SIX6	SCG5
	HOXD10	SCG5	DACH1	PPP2R2B
		LUM	PPP2R2C	DACH1
		PPP2R2C	DKK1	DKK1
		ROBO2	TNFAIP6	RET
		DKK1	RET	PRKCA
		RET	PRKCA	

Table 4

Table of significant transcripts for testing “Class 3R vs. 4R” main effect (102 transcripts were found significant at level 0.001)

RefSeq transcript ID	Gene symbol	Entrez Gene name	p-value
NM_174941	CD163L1	Homo sapiens CD163 molecule-like 1 (CD163L1), mRNA.	0.00E+00
NM_032048	EMILIN2	Homo sapiens elastin microfibril interfacer 2 (EMILIN2), mRNA.	0.00E+00
NM_207334	FAM43B	Homo sapiens family with sequence similarity 43, member B (FAM43B), mRNA.	0.00E+00
NM_144594	GTSF1	Homo sapiens gametocyte specific factor 1 (GTSF1), mRNA.	0.00E+00
NM_005519	HMX2	Homo sapiens H6 family homeobox 2 (HMX2), mRNA.	0.00E+00
AB073882	Hs.1832	Homo sapiens primary neuroblastoma cDNA, clone:Nbla00830, full insert sequence	0.00E+00
NM_021048	MAGEA10	Homo sapiens melanoma antigen family A, 10 (MAGEA10), transcript variant 2, mRNA.	0.00E+00
NM_000905	NPY	Homo sapiens neuropeptide Y (NPY), mRNA.	0.00E+00
XM_001133042	PDZRN3	PREDICTED: Homo sapiens PDZ domain containing RING finger 3 (PDZRN3), mRNA.	0.00E+00
XM_001133042	PDZRN3	PREDICTED: Homo sapiens PDZ domain containing RING finger 3 (PDZRN3), mRNA.	0.00E+00
NM_002942	ROBO2	Homo sapiens roundabout, axon guidance receptor, homolog 2 (Drosophila) (ROBO2), mRNA.	0.00E+00
NR_002784	SMEK3P	Homo sapiens SMEK homolog 3, suppressor of mek1 (Dictyostelium) pseudogene (SMEK3P) on chromosome X.	0.00E+00
NM_007115	TNFAIP6	Homo sapiens tumor necrosis factor, alpha-induced protein 6 (TNFAIP6), mRNA.	0.00E+00
NM_018027	FRMD4A	Homo sapiens FERM domain containing 4A (FRMD4A), mRNA.	0.00E+00
NM_001769	CD9	Homo sapiens CD9 molecule (CD9), mRNA.	0.00E+00
NM_002334	LRP4	Homo sapiens low density lipoprotein receptor-related protein 4 (LRP4), mRNA.	0.00E+00
NM_017637	BNC2	Homo sapiens basonuclin 2 (BNC2), mRNA.	0.00E+00
NM_139072	DNER	Homo sapiens delta/notch-like EGF repeat containing (DNER), mRNA.	0.00E+00
NM_000624	SERPINA5	Homo sapiens serpin peptidase inhibitor, clade A (alpha-1 antiproteinase, antitrypsin), member 5 (SERPINA5), mRNA.	0.00E+00
NM_003020	SCG5	Homo sapiens secretogranin V (7B2 protein) (SCG5), mRNA.	0.00E+00
NM_194435	VIP	Homo sapiens vasoactive intestinal peptide (VIP), transcript variant 2, mRNA.	0.00E+00
NM_018286	TMEM100	Homo sapiens transmembrane protein 100 (TMEM100), transcript variant 2, mRNA.	0.00E+00
NM_020975	RET	Homo sapiens ret proto-oncogene (RET), transcript variant 2, mRNA.	0.00E+00
NM_013364	PNMA3	Homo sapiens paraneoplastic antigen MA3 (PNMA3), mRNA.	0.00E+00
NM_002737	PRKCA	Homo sapiens protein kinase C, alpha (PRKCA), mRNA.	0.00E+00
NM_001290	LDB2	Homo sapiens LIM domain binding 2 (LDB2), mRNA.	0.00E+00
BX537518	Hs.7023	Homo sapiens mRNA; cDNA DKFZp686N1989 (from clone DKFZp686N1989)	0.00E+00
NM_001013653	LRRC26	Homo sapiens leucine rich repeat containing 26 (LRRC26), mRNA.	0.00E+00
NM_001453	FOXC1	Homo sapiens forkhead box C1 (FOXC1), mRNA.	0.00E+00
NM_182801	EGFLAM	Homo sapiens EGF-like, fibronectin type III and laminin G domains (EGFLAM), transcript variant 4, mRNA.	0.00E+00
NM_004100	EYA4	Homo sapiens eyes absent homolog 4 (Drosophila) (EYA4), transcript variant 1, mRNA.	0.00E+00
NM_201630	LRRN2	Homo sapiens leucine rich repeat neuronal 2 (LRRN2), transcript variant 2, mRNA.	0.00E+00
NM_080760	DACH1	Homo sapiens dachshund homolog 1 (Drosophila) (DACH1), transcript variant 2, mRNA.	0.00E+00
NM_152330	FRMD6	Homo sapiens FERM domain containing 6 (FRMD6), transcript variant 2, mRNA.	0.00E+00
NM_173662	RNF175	Homo sapiens ring finger protein 175 (RNF175), mRNA.	0.00E+00
NM_013322	SNX10	Homo sapiens sorting nexin 10 (SNX10), mRNA.	0.00E+00

RefSeq transcript ID	Gene symbol	Entrez Gene name	p-value
NM_001613	ACTA2	Homo sapiens actin, alpha 2, smooth muscle, aorta (ACTA2), mRNA.	0.00E+00
NM_001001995	GPM6B	Homo sapiens glycoprotein M6B (GPM6B), transcript variant 1, mRNA.	0.00E+00
NM_003283	TNNT1	Homo sapiens troponin T type 1 (skeletal, slow) (TNNT1), mRNA.	0.00E+00
NM_001915	CYB561	Homo sapiens cytochrome b-561 (CYB561), transcript variant 1, mRNA.	0.00E+00
NM_033258	GNG8	Homo sapiens guanine nucleotide binding protein (G protein), gamma 8 (GNG8), mRNA.	0.00E+00
NM_002148	HOXD10	Homo sapiens homeobox D10 (HOXD10), mRNA.	0.00E+00
NM_057159	LPAR1	Homo sapiens lysophosphatidic acid receptor 1 (LPAR1), transcript variant 2, mRNA.	0.00E+00
NM_001946	DUSP6	Homo sapiens dual specificity phosphatase 6 (DUSP6), transcript variant 1, mRNA.	0.00E+00
NM_145764	MGST1	Homo sapiens microsomal glutathione S-transferase 1 (MGST1), transcript variant 1d, mRNA.	0.00E+00
NM_018962	DSCR6	Homo sapiens Down syndrome critical region gene 6 (DSCR6), mRNA.	0.00E+00
NM_014141	CNTNAP2	Homo sapiens contactin associated protein-like 2 (CNTNAP2), mRNA.	0.00E+00
NM_002872	RAC2	Homo sapiens ras-related C3 botulinum toxin substrate 2 (rho family, small GTP binding protein Rac2) (RAC2), mRNA.	0.00E+00
NM_020826	SYT13	Homo sapiens synaptotagmin XIII (SYT13), mRNA.	0.00E+00
NM_001039582	PNCK	Homo sapiens pregnancy upregulated non-ubiquitously expressed CaM kinase (PNCK), mRNA.	0.00E+00
NM_020630	RET	Homo sapiens ret proto-oncogene (RET), transcript variant 4, mRNA.	0.00E+00
NM_003619	PRSS12	Homo sapiens protease, serine, 12 (neurotrypsin, motopsin) (PRSS12), mRNA.	0.00E+00
NM_006157	NELL1	Homo sapiens NEL-like 1 (chicken) (NELL1), mRNA.	0.00E+00
NM_014817	KIAA0644	Homo sapiens KIAA0644 gene product (KIAA0644), mRNA.	0.00E+00
XM_939093	FAM89A	PREDICTED: Homo sapiens family with sequence similarity 89, member A (FAM89A), mRNA.	0.00E+00
NM_181876	PPP2R2C	protein phosphatase 2, subunit B, gamma isoform (PPP2R2C), transcript variant 2, mRNA.	0.00E+00
NM_012242	DKK1	Homo sapiens dickkopf homolog 1 (Xenopus laevis) (DKK1), mRNA.	0.00E+00
NM_006017	PROM1	Homo sapiens prominin 1 (PROM1), mRNA.	0.00E+00
BX100246	Hs.38132	BX100246 Soares fetal liver spleen 1NFLS Homo sapiens cDNA clone IMAGp998N04398, mRNA sequence	0.00E+00
NM_001001995	GPM6B	Homo sapiens glycoprotein M6B (GPM6B), transcript variant 1, mRNA.	0.00E+00
NM_002345	LUM	Homo sapiens lumican (LUM), mRNA.	0.00E+00
NM_007374	SIX6	Homo sapiens SIX homeobox 6 (SIX6), mRNA.	0.00E+00
NM_181676	PPP2R2B	Homo sapiens protein phosphatase 2 (formerly 2A), regulatory subunit B, beta isoform (PPP2R2B), transcript variant 4, mRNA.	0.00E+00
NM_005627	SGK	Homo sapiens serum/glucocorticoid regulated kinase (SGK), mRNA.	0.00E+00
NM_020975	RET	Homo sapiens ret proto-oncogene (RET), transcript variant 2, mRNA.	0.00E+00
NM_020775	KIAA1324	Homo sapiens KIAA1324 (KIAA1324), mRNA.	0.00E+00
NM_002930	RIT2	Homo sapiens Ras-like without CAAX 2 (RIT2), mRNA.	0.00E+00
NM_080390	TCEAL2	Homo sapiens transcription elongation factor A (SII)-like 2 (TCEAL2), mRNA.	0.00E+00
NM_021170	HES4	Homo sapiens hairy and enhancer of split 4 (Drosophila) (HES4), mRNA.	0.00E+00
NM_001475	GAGE5	Homo sapiens G antigen 5 (GAGE5), mRNA.	0.00E+00
NM_130467	PAGE5	Homo sapiens P antigen family, member 5 (prostate associated) (PAGE5), transcript variant 1, mRNA.	0.00E+00
NM_004431	EPHA2	Homo sapiens EPH receptor A2 (EPHA2), mRNA.	0.00E+00
NM_182898	CREB5	Homo sapiens cAMP responsive element binding protein 5 (CREB5), transcript variant 1, mRNA.	0.00E+00

RefSeq transcript ID	Gene symbol	Entrez Gene name	p-value
NM_001476	GAGE6	Homo sapiens G antigen 6 (GAGE6), mRNA.	0.00E+00
NM_001475	GAGE5	Homo sapiens G antigen 5 (GAGE5), mRNA.	0.00E+00
NM_001099660	LRRN3	Homo sapiens leucine rich repeat neuronal 3 (LRRN3), transcript variant 1, mRNA.	0.00E+00
NM_004192	ASMTL	Homo sapiens acetylserotonin O-methyltransferase-like (ASMTL), mRNA.	0.00E+00
NM_004192	ASMTL	Homo sapiens acetylserotonin O-methyltransferase-like (ASMTL), mRNA.	0.00E+00
NM_001474	GAGE4	Homo sapiens G antigen 4 (GAGE4), mRNA.	0.00E+00
NM_020822	KCNT1	Homo sapiens potassium channel, subfamily T, member 1 (KCNT1), mRNA.	0.00E+00
NM_001098409	GAGE12G	Homo sapiens G antigen 12G (GAGE12G), mRNA.	0.00E+00
XM_938742	SGPP2	PREDICTED: Homo sapiens sphingosine-1-phosphate phosphotase 2 (SGPP2), mRNA.	0.00E+00
NM_014550	CARD10	Homo sapiens caspase recruitment domain family, member 10 (CARD10), mRNA.	0.00E+00
NM_001098411	LOC645037	Homo sapiens similar to GAGE-2 protein (G antigen 2) (LOC645037), mRNA.	0.00E+00
NM_001477	GAGE12I	Homo sapiens G antigen 12I (GAGE12I), mRNA.	0.00E+00
NM_004617	TM4SF4	Homo sapiens transmembrane 4 L six family member 4 (TM4SF4), mRNA.	1.00E−04
NM_012202	GNG3	Homo sapiens guanine nucleotide binding protein (G protein), gamma 3 (GNG3), mRNA.	1.00E−04
NM_014220	TM4SF1	Homo sapiens transmembrane 4 L six family member 1 (TM4SF1), mRNA.	1.00E−04
NM_001031733	CALML4	Homo sapiens calmodulin-like 4 (CALML4), transcript variant 2, mRNA.	1.00E−04
NM_020116	FSTL5	Homo sapiens follistatin-like 5 (FSTL5), mRNA.	2.00E−04
NM_006528	TFPI2	Homo sapiens tissue factor pathway inhibitor 2 (TFPI2), mRNA.	2.00E−04
NM_207336	ZNF467	Homo sapiens zinc finger protein 467 (ZNF467), mRNA.	2.00E−04
NM_004864	GDF15	Homo sapiens growth differentiation factor 15 (GDF15), mRNA.	2.00E−04
NM_152780	MAP7D2	Homo sapiens MAP7 domain containing 2 (MAP7D2), mRNA.	3.00E−04
NM_133505	DCN	Homo sapiens decorin (DCN), transcript variant C, mRNA.	3.00E−04
NM_022450	RHBDF1	Homo sapiens rhomboid 5 homolog 1 (Drosophila) (RHBDF1), mRNA.	3.00E−04
NM_172081	CAMK2B	Homo sapiens calcium/calmodulin-dependent protein kinase (CaM kinase) II beta (CAMK2B), transcript variant 5, mRNA.	4.00E−04
NM_177526	PPAP2C	Homo sapiens phosphatidic acid phosphatase type 2C (PPAP2C), transcript variant 2, mRNA.	5.00E−04
NM_000582	SPP1	Homo sapiens secreted phosphoprotein 1 (SPP1), transcript variant 2, mRNA.	6.00E−04
NM_183337	RGS11	Homo sapiens regulator of G-protein signaling 11 (RGS11), transcript variant 1, mRNA.	7.00E−04
NM_194439	RNF212	Homo sapiens ring finger protein 212 (RNF212), mRNA.	8.00E−04
NM_002414	CD99	Homo sapiens CD99 molecule (CD99), transcript variant 1, mRNA.	9.00E−04

Table 5

Table of significant transcripts for testing “Class 2N vs. 0N” main effect (56 transcripts were found significant at level 0.001)

RefSeq transcript ID	Gene symbol	Entrez Gene name	p-value
NM_002334	LRP4	Homo sapiens low density lipoprotein receptor-related protein 4 (LRP4), mRNA.	0.00E+00
XM_939093	FAM89A	PREDICTED: Homo sapiens family with sequence similarity 89, member A (FAM89A), mRNA.	0.00E+00
NM_001769	CD9	Homo sapiens CD9 molecule (CD9), mRNA.	0.00E+00
NM_018286	TMEM100	Homo sapiens transmembrane protein 100 (TMEM100), transcript variant 2, mRNA.	0.00E+00
NM_182898	CREB5	Homo sapiens cAMP responsive element binding protein 5 (CREB5), transcript variant 1, mRNA.	0.00E+00
NM_020975	RET	Homo sapiens ret proto-oncogene (RET), transcript variant 2, mRNA.	0.00E+00
NM_018027	FRMD4A	Homo sapiens FERM domain containing 4A (FRMD4A), mRNA.	0.00E+00
NM_007115	TNFAIP6	Homo sapiens tumor necrosis factor, alpha-induced protein 6 (TNFAIP6), mRNA.	0.00E+00
NM_001613	ACTA2	Homo sapiens actin, alpha 2, smooth muscle, aorta (ACTA2), mRNA.	0.00E+00
NM_182801	EGFLAM	Homo sapiens EGF-like, fibronectin type III and laminin G domains (EGFLAM), transcript variant 4, mRNA.	0.00E+00
NM_002942	ROBO2	Homo sapiens roundabout, axon guidance receptor, homolog 2 (Drosophila) (ROBO2), mRNA.	0.00E+00
NM_000905	NPY	Homo sapiens neuropeptide Y (NPY), mRNA.	0.00E+00
NM_004100	EYA4	Homo sapiens eyes absent homolog 4 (Drosophila) (EYA4), transcript variant 1, mRNA.	0.00E+00
NM_000582	SPP1	Homo sapiens secreted phosphoprotein 1 (SPP1), transcript variant 2, mRNA.	0.00E+00
NM_194435	VIP	Homo sapiens vasoactive intestinal peptide (VIP), transcript variant 2, mRNA.	0.00E+00
NM_017637	BNC2	Homo sapiens basonuclin 2 (BNC2), mRNA.	0.00E+00
NM_014141	CNTNAP2	Homo sapiens contactin associated protein-like 2 (CNTNAP2), mRNA.	0.00E+00
NM_003619	PRSS12	Homo sapiens protease, serine, 12 (neurotrypsin, motopsin) (PRSS12), mRNA.	0.00E+00
NM_022450	RHBDF1	Homo sapiens rhomboid 5 homolog 1 (Drosophila) (RHBDF1), mRNA.	0.00E+00
NM_001475	GAGE5	Homo sapiens G antigen 5 (GAGE5), mRNA.	0.00E+00
NM_033258	GNG8	Homo sapiens guanine nucleotide binding protein (G protein), gamma 8 (GNG8), mRNA.	0.00E+00
NM_001477	GAGE12I	Homo sapiens G antigen 12I (GAGE12I), mRNA.	0.00E+00
NM_001098411	LOC645037	Homo sapiens similar to GAGE-2 protein (G antigen 2) (LOC645037), mRNA.	0.00E+00
NM_001476	GAGE6	Homo sapiens G antigen 6 (GAGE6), mRNA.	0.00E+00
NM_145764	MGST1	Homo sapiens microsomal glutathione S-transferase 1 (MGST1), transcript variant 1d, mRNA.	0.00E+00
NM_001474	GAGE4	Homo sapiens G antigen 4 (GAGE4), mRNA.	0.00E+00
NM_001946	DUSP6	Homo sapiens dual specificity phosphatase 6 (DUSP6), transcript variant 1, mRNA.	0.00E+00
NM_002930	RIT2	Homo sapiens Raslike without CAAX 2 (RIT2), mRNA.	0.00E+00
NM_002737	PRKCA	Homo sapiens protein kinase C, alpha (PRKCA), mRNA.	0.00E+00
NM_002213	ITGB5	Homo sapiens integrin, beta 5 (ITGB5), mRNA. XM_944688 XM_944693	0.00E+00
NM_001475	GAGE5	Homo sapiens G antigen 5 (GAGE5), mRNA.	0.00E+00
NM_004864	GDF15	Homo sapiens growth differentiation factor 15 (GDF15), mRNA.	0.00E+00
BX100246	Hs.38132	BX100246 Soares fetal liver spleen 1NFLS Homo sapiens cDNA clone IMAGp998N0 4398, mRNA sequence	0.00E+00
AB073882	Hs.1832	Homo sapiens primary neuroblastoma cDNA, clone:Nbla00830, full insert sequence	0.00E+00

RefSeq transcript ID	Gene symbol	Entrez Gene name	p-value
NM_006017	PROM1	Homo sapiens prominin 1 (PROM1), mRNA.	0.00E+00
NM_002345	LUM	Homo sapiens lumican (LUM), mRNA.	0.00E+00
NM_001098409	GAGE12G	Homo sapiens G antigen 12G (GAGE12G), mRNA.	0.00E+00
NM_020630	RET	Homo sapiens ret proto-oncogene (RET), transcript variant 4, mRNA.	0.00E+00
NM_002414	CD99	Homo sapiens CD99 molecule (CD99), transcript variant 1, mRNA.	1.00E−04
NM_001915	CYB561	Homo sapiens cytochrome b-561 (CYB561), transcript variant 1, mRNA.	1.00E−04
NM_057159	LPAR1	Homo sapiens lysophosphatidic acid receptor 1 (LPAR1), transcript variant 2, mRNA.	1.00E−04
NM_003283	TNNT1	Homo sapiens troponin T type 1 (skeletal, slow) (TNNT1), mRNA.	1.00E−04
NM_020975	RET	Homo sapiens ret proto-oncogene (RET), transcript variant 2, mRNA.	1.00E−04
NM_001031733	CALML4	Homo sapiens calmodulin-like 4 (CALML4), transcript variant 2, mRNA.	1.00E−04
NM_013364	PNMA3	Homo sapiens paraneoplastic antigen MA3 (PNMA3), mRNA.	1.00E−04
NM_014220	TM4SF1	Homo sapiens transmembrane 4 L six family member 1 (TM4SF1), mRNA.	1.00E−04
NM_032048	EMILIN2	Homo sapiens elastin microfibril interfacer 2 (EMILIN2), mRNA.	2.00E−04
XM_001132569	LOC730130	PREDICTED: Homo sapiens hypothetical protein LOC730130 (LOC730130), mRNA.	2.00E−04
NM_004617	TM4SF4	Homo sapiens transmembrane 4 L six family member 4 (TM4SF4), mRNA.	3.00E−04
NM_001001391	CD44	Homo sapiens CD44 molecule (Indian blood group) (CD44), transcript variant 4, mRNA.	3.00E−04
NM_023940	RASL11B	Homo sapiens RAS-like, family 11, member B (RASL11B), mRNA.	4.00E−04
NM_130467	PAGE5	Homo sapiens P antigen family, member 5 (prostate associated) (PAGE5), transcript variant 1, mRNA.	4.00E−04
NM_144594	GTSF1	Homo sapiens gametocyte specific factor 1 (GTSF1), mRNA.	5.00E−04
NM_194439	RNF212	Homo sapiens ring finger protein 212 (RNF212), mRNA.	6.00E−04
NM_006528	TFPI2	Homo sapiens tissue factor pathway inhibitor 2 (TFPI2), mRNA.	8.00E−04
BX537518	Hs.7023	Homo sapiens mRNA; cDNA DKFZp686N1989 (from clone DKFZp686N1989)	9.00E−04

J Alzheimers Dis. Author manuscript; available in PMC 2012 April 10.

Table 6

Significant ANOVA interactions between 0N/2N and 3R/4R Classes

RefSeq transcript ID	Gene symbol	Mean[1] 4R/2N (A)	Mean[1] 3R/2N (B)	Mean[1] 4R/0N (C)	Mean[1] 3R/0N (D)
NM_000685	AGTR1	6.02	6.44	7.63	5.93
NM_004192	ASMTL	8.92	6.50	7.85	7.61
NM_018354	C20orf46	9.39	6.71	8.04	8.42
NM_002414	CD99	5.26	5.54	9.10	5.72
NM_014141	CNTNAP2	10.81	7.06	7.79	6.54
NM_133505	DCN	5.51	7.57	5.81	5.77
NM_012242	DKK1	8.30	12.18	9.92	10.92
NM_001387	DPYSL3	8.84	9.25	9.50	7.85
NM_001430	EPAS1	6.33	8.65	8.64	7.87
NM_144967	ARHGAP36	6.35	7.43	8.08	5.92
NM_001458	FLNC	7.83	6.45	5.81	7.33
NM_001001995	GPM6B	8.91	9.30	7.62	9.52
NM_003918	GYG2	5.37	5.69	7.11	5.50
NR_002196	H19	11.47	13.03	13.45	11.78
AK095715	Hs.155736	5.67	7.58	7.70	6.66
CD678339	TMEM229A	8.28	9.64	9.80	9.34
NM_000598	IGFBP3	5.53	7.66	6.07	5.56
NM_002213	ITGB5	5.92	6.39	7.64	6.56
NM_020822	KCNT1	9.99	6.48	7.75	7.43
NM_152780	MAP7D2	8.43	6.37	8.17	8.21
NM_024019	NEUROG2	5.68	9.88	7.72	6.47
NM_181689	NNAT	9.23	11.75	11.61	11.30
NM_005386	NNAT	6.39	9.02	8.86	8.46
NM_130467	PAGE5	6.02	5.57	9.03	5.45
NM_080390	TCEAL2	8.92	6.05	6.76	6.30
NM_003598	TEAD2	5.45	8.72	8.60	5.85
NM_004617	TM4SF4	5.34	8.41	5.40	5.52
NM_002166	ID2	8.80	10.29	10.19	8.43

RefSeq transcript ID	Gene symbol	Mean[1] 4R/2N (A)	Mean[1] 3R/2N (B)	Mean[1] 4R/0N (C)	Mean[1] 3R/0N (D)
NM_080415	4-Sep	8.36	6.50	6.83	7.38
NM_000316	PTH1R	7.84	6.17	6.56	6.70
NM_032594	INSM2	9.63	11.50	11.23	10.89
NM_001001391	CD44	5.74	7.57	5.77	5.52
NM_032808	LINGO1	7.53	5.95	7.12	7.37
NM_006157	NELL1	6.89	6.37	7.85	6.07
NM_194439	RNF212	7.11	5.37	5.35	5.47
NM_020826	SYT13	8.65	6.31	7.53	6.74
NM_000419	ITGA2B	8.09	6.63	6.73	7.35
NM_033258	GNG8	5.90	8.84	8.04	9.11
XM_001132569	LOC730130	6.55	7.79	8.25	7.78
NM_012202	GNG3	9.88	6.83	7.48	7.36
NM_003161	FAM20C	7.38	5.80	5.90	6.09
NM_004192	ASMTL	8.37	6.16	7.52	7.29
NM_001099660	LRRN3	8.29	10.03	9.29	9.50
NM_194435	VIP	6.27	10.53	5.84	8.23
NM_020775	KIAA1324	7.49	5.47	6.04	5.66
NM_020851	ISLR2	7.61	8.51	9.52	8.24
NM_014220	TM4SF1	5.27	6.37	5.23	5.28
NM_001031733	CALML4	8.88	8.90	7.76	8.86
NM_005627	SGK1	7.45	7.11	8.45	6.68
NM_032229	SLITRK6	5.52	7.28	7.01	6.58
NM_057159	LPAR1	7.23	9.50	7.15	7.96
NM_181676	PPP2R2B	9.48	7.61	8.93	8.56
NM_001039582	PNCK	9.85	7.70	9.21	8.51
NM_000728	CALCB	9.55	8.24	8.15	8.72
NM_002148	HOXD10	6.06	6.97	5.94	8.45
NM_174947	C19ORF30	7.65	6.17	6.25	6.66
NM_023940	RASL11B	7.69	8.79	8.94	8.76
NM_012155	EML2	9.94	8.17	8.73	8.97
NM_033504	TMEM54	7.68	6.14	6.42	6.79

RefSeq transcript ID	Gene symbol	Mean[1] 4R/2N (A)	Mean[1] 3R/2N (B)	Mean[1] 4R/0N (C)	Mean[1] 3R/0N (D)
NM_001476	GAGE6	5.36	5.51	5.51	6.69
NM_181876	PPP2R2C	8.52	6.10	7.81	7.12
NM_003053	SLC18A1	7.38	7.62	8.81	7.28
NM_177526	PPAP2C	8.54	6.92	8.04	8.10
NM_007374	SIX6	8.55	6.21	7.20	6.72
XM_938742	SGPP2	7.45	7.59	6.17	7.82
NR_003512	UBE2J2	5.68	6.79	7.82	5.79
NM_000582	SPP1	5.72	6.88	5.44	5.39
NM_002872	RAC2	7.06	5.56	6.22	5.70
NM_002224	ITPR3	8.19	6.72	6.73	7.38
NM_014550	CARD10	7.51	5.94	6.46	6.31
NM_207336	ZNF467	6.66	5.34	5.54	5.52
NM_004864	GDF15	8.23	6.85	6.68	6.68
NM_001290	LDB2	8.07	5.94	7.52	6.43
NM_000624	SERPINA5	9.21	5.91	8.81	6.84
NM_018286	TMEM100	8.97	9.80	9.68	11.22
NM_015557	CHD5	7.90	6.17	6.11	6.36
NM_002345	LUM	5.76	7.31	5.64	5.98
CN304251	Hs.436189	8.18	5.89	7.27	7.47
NM_172081	CAMK2B	9.60	7.79	8.88	8.92
NM_080760	DACH1	6.85	9.57	7.74	9.00
NM_013322	SNX10	9.13	6.96	8.34	7.38
NM_018962	DSCR6	7.75	5.94	6.69	6.04
BX100246	Hs.38132	6.02	7.48	5.89	6.26
NM_021170	HES4	10.17	8.26	8.91	8.60
NM_004431	EPHA2	8.62	6.99	7.55	7.32
NM_001453	FOXC1	6.68	8.94	7.73	8.85
NM_022450	RHBDF1	7.04	5.99	5.76	5.77
NM_020975	RET	5.90	7.14	6.95	7.21
NM_152330	FRMD6	6.71	8.43	6.96	7.75
NM_006528	TFPI2	7.06	7.01	8.67	6.93

RefSeq transcript ID	Gene symbol	Mean[1] 4R/2N (A)	Mean[1] 3R/2N (B)	Mean[1] 4R/0N (C)	Mean[1] 3R/0N (D)
NM_201630	LRRN2	7.80	5.76	6.92	5.96
NM_001013653	LRRC26	8.92	6.35	8.23	6.93
NM_001474	GAGE7	5.24	5.41	5.43	6.69
NM_014817	TRIL	8.01	9.73	8.16	8.69
NM_001475	GAGE7	5.27	5.47	5.43	6.66
NM_183337	RGS11	9.75	7.64	8.15	8.21
NM_182801	EGFLAM	7.59	6.34	6.71	6.08
NM_001098409	GAGE6	5.41	5.55	5.53	6.75
NM_001001995	GPM6B	6.92	7.68	6.09	7.90
NM_013364	PNMA3	9.28	6.77	8.04	6.69
NM_004100	EYA4	6.59	8.30	6.30	7.16
NM_006017	PROM1	5.54	6.68	5.43	5.74
NM_000787	DBH	11.04	12.34	12.60	12.10
NM_001477	GAGE12I	5.19	5.31	5.39	6.55
NM_001946	DUSP6	6.13	7.46	7.09	7.60
NM_002930	RIT2	6.88	5.66	5.76	5.50
NM_001475	GAGE7	5.45	5.64	5.67	6.90
NM_001915	CYB561	9.21	8.61	10.19	8.69
NM_145764	MGST1	8.21	6.71	8.39	7.82
NM_020116	FSTL5	8.11	6.84	6.96	6.88
NM_173662	RNF175	8.68	6.66	7.99	7.05
NM_001098411	GAGE2B	5.38	5.52	5.58	6.71
NM_003020	SCG5	11.59	9.96	11.47	10.48
NM_020630	RET	6.77	8.19	7.80	8.31
NM_003619	PRSS12	7.92	9.31	7.66	8.15
NM_003283	TNNT1	9.89	8.03	10.01	9.23
NM_020975	RET	6.60	8.12	7.71	8.57
NR_003655	POLR2J4	5.85	7.38	7.37	5.72
NM_207334	FAM43B	8.03	5.71	7.71	5.89
NM_139072	DNER	7.47	5.52	7.12	5.86
NM_018027	FRMD4A	7.94	6.72	7.62	5.91

RefSeq transcript ID	Gene symbol	Mean[1] 4R/2N (A)	Mean[1] 3R/2N (B)	Mean[1] 4R/0N (C)	Mean[1] 3R/0N (D)
BX537518	LOC100130155	6.62	5.01	5.89	5.00
NM_001613	ACTA2	7.95	6.58	6.84	6.18
NM_017637	BNC2	5.48	7.00	5.29	6.31
NM_005519	HMX2	5.48	7.98	5.50	7.60
NM_000905	NPY	12.53	9.22	12.19	8.23
NM_174941	CD163L1	7.56	5.93	7.93	5.91
NM_182898	CREB5	9.37	9.63	7.91	8.95
NM_002737	PRKCA	8.89	9.81	9.09	10.62
XM_939093	FAM89A	7.42	6.51	5.88	5.49

[1] Signal intensity values log2 transformed.